ACS ES&T Engineering

pubs.acs.org/estengg

Article

Counterion Mobility in Ion-Exchange Membranes: Spatial Effect and Valency-Dependent Electrostatic Interaction

Hanqing Fan, Yuxuan Huang, Ian H. Billinge, Sean M. Bannon, Geoffrey M. Geise, and Ngai Yin Yip*

Cite This: *ACS EST Engg.* 2022, 2, 1274–1286

Read Online

ACCESS | Metrics & More | Article Recommendations | Supporting Information

ABSTRACT: Enhancing the selectivity of ion-exchange membranes (IEMs) is an important need for environmental separations but is hindered by insufficient understanding of the fundamental transport phenomena. Specifically, existing models do not adequately explain the order of magnitude disparity in diffusivities of mono-, di-, and trivalent ions within the membranes. In this study, a transport framework is presented to describe counterion migration mobility using an analytical expression based on first-principles. The two governing mechanisms are spatial effect of available fractional volume for ion transport and electrostatic interaction between mobile ions and fixed charges. Mobilities of counterions with different valencies were experimentally characterized and shown to have high R^2s in regression analyses with the proposed transport model. The influence of membrane swelling caused by different counterions was further accounted for to better model the spatial effect. The frictional effect of electrostatic interaction was quantitatively linked to the membrane structural and electrical properties of fixed charged density and dielectric constant. Additionally, the anion-exchange membrane exhibited a weaker electrostatic effect compared to cation-exchange membranes, which was attributed to steric hindrance caused by hydrocarbon chains of the quaternary amine functional groups. The insights offered in this study can inform the rational development of IEMs and membrane processes for ion-specific separations.

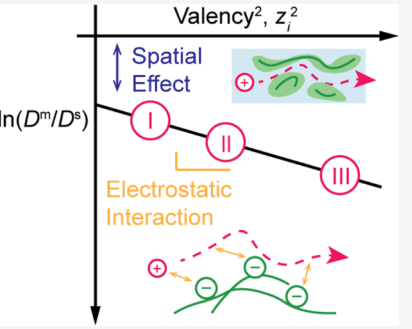

KEYWORDS: *ion-exchange membranes, counterion mobility, ion valency, diffusivity, transport selectivity*

INTRODUCTION

Improved selectivity in separations has been identified as a critical need for water, energy, and environment.[1−3] Fractionation of like-charged ions is required for several environmentally important separations. For example, the selective recoveries of nitrogenous compounds and orthophosphates from wastewaters with complex ionic compositions are vital to enable nutrient recycling (i.e., differentiating NO_3^- and $H_xPO_4^{3-x}$ anions from Cl^-, HCO_3^-, and SO_4^{2-} and discriminating between NH_4^+ and other cations of Na^+, Ca^{2+}, and Mg^{2+}).[4−6] Likewise, the precise removal of trace contaminants from much higher concentrations of background ions (such as Pb^{2+}, Hg^{2+}, Cd^{2+}, and Cr^{2+} cations from Na^+, K^+, Ca^{2+}, and Mg^{2+} and anions of $H_2AsO_4^-$, $H_2BO_3^-$, and SeO_4^{2-} from Cl^-, HCO_3^-, and SO_4^{2-}) is pivotal for water security.[2,7−9] The targeted extraction of Li^+ from other cations (e.g., Na^+, K^+, Ca^{2+}, and Mg^{2+}) can realize the economic harvesting of lithium, a critical element in batteries, from unconventional sources, such as oil and gas produced water.[10]

Ion-exchange membranes (IEMs) are highly charged polymeric thin films primarily used in electrodialysis for brackish water desalination, chloralkali process for electrolytic manufacture of $Cl_{2(g)}$ and $NaOH_{(aq)}$, and electrodeionization for ultrapure water production.[11−13] The membranes are also employed in energy applications, such as fuel cells and reverse electrodialysis.[14−19] These IEM processes utilize charged membranes as barriers to allow the transport of oppositely charged counterions while retaining like-charged co-ions (and water). Recently, there is an increasing interest in using IEMs for separation of like-charged species, that is, beyond discrimination between counter- and co-ions.[20−24] Fundamental understanding of the transport mechanisms is imperative to inform the development of ion-selective IEMs and separation processes,[21,22] and there has been much research to that end.[20,22,23]

The theoretical framework to quantitatively relate ion mobilities to membrane parameters and ion properties is underdeveloped and represents a critical knowledge gap. Mobility is the ion drift velocity under an electric field and is related to diffusivity through the Einstein relation.[11,25] Ion transport proceeds as sorption into the membrane followed by electromigration or diffusion across the IEM, driven by an electric or chemical potential gradient, respectively.[11,26,27] Counterion mobility is, therefore, of key importance for determining selectivity between like-charged counterions.[11,28]

Received: November 30, 2021
Revised: February 17, 2022
Accepted: February 23, 2022
Published: March 10, 2022

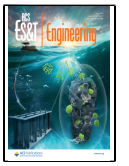

Significant progress has been achieved by previous studies to elucidate the general factors influencing ion mobility in IEMs. For example, the membrane properties of water uptake,[29−32] fixed charge density,[31,33] and nano/microscale structures[34−36] have been reported to affect IEM counterion mobility (or equivalently, conductivity). Counterion properties of size,[32,37] valency,[29,32,38−40] hydration energy,[41] and Lewis acid strength[32] were also found to influence mobility. However, these past studies are largely phenomenological or qualitative assessments. The counterion condensation theory is one of the handful of quantitative approaches that has been applied to IEMs to obtain predictions for activity coefficients and co-ion-dominated salt permeabilities.[42,43] However, the existing framework does not account for counterion mobility in the condensed phase, which was recently shown to be a significant contributor to net ion fluxes.[44] An alternative approach incorporates molecular frictions between different species, based on the Maxwell−Stefan theory, into the Nernst−Planck framework.[16,45−47] However, hindrance factors for the molecular frictions, which are at the center of the model, are not readily available *a priori*. The deficiencies in the understanding of ion mobility impede the development of membranes and IEM separations capable of better distinguishing between different counterions. As such, there is a need to further advance first-principles-based models for counterion mobility.

This study integrates theoretical analysis with experimental investigation to examine counterion mobility in IEMs. First, a transport model is presented to describe counterion diffusivity in IEMs. The model is based on the two primary phenomena of spatial effect of sorbed water and electrostatic interaction between mobile ions and fixed charges. Specifically, the spatial effect of membrane water content on ion diffusivity was quantified using the Mackie−Meares approach, whereas the electrostatic effect induced by membrane fixed charges was modeled as migration of the mobile counterions down a rough electric potential gradient. Following the construction of the model, transport experiments were conducted to investigate the principal factors influencing counterion diffusivity. Conductivities of different mono-, di-, and trivalent counterions in three commercial cation-exchange membranes (CEMs) and one anion-exchange membrane (AEM) were experimentally characterized to determine the ion diffusivities in different IEMs. The impact of counterion-dependent membrane swelling on diffusivity was then assessed using different electrolyte solutions. The frictional effect of electrostatic interaction was quantitatively related to the membrane structural and electrical properties of fixed charged density and effective dielectric constant. Discussion then moves to the role of charged functional groups in the weaker electrostatic effect observed in the AEM. Next, we review other relevant ion-transport models and theories, such as ion dehydration, activated diffusion, Onsager's relationship, and counterion condensation, in relation to the framework presented here. Last, the implications of the counterion mobility transport model for ion-selective separations are discussed.

■ ION-TRANSPORT MODEL THEORY

Membrane Conductivity, Ion Mobility, and Diffusivity. For typical IEM processes where migration driven by an applied electric potential dominates transport, the membrane ionic conductivity, σ, can be related to the ion mobility, u, or diffusivity, D, by[11,25]

$$\sigma = F\sum |z_i| c_i^{\mathrm{m}} u_i^{\mathrm{m}} = \frac{F^2}{R_{\mathrm{g}}T}\sum z_i^2 c_i^{\mathrm{m}} D_i^{\mathrm{m}} \tag{1}$$

where z is the ion valency, c is the molar concentration, F is Faraday constant, R_{g} is the ideal gas constant, and T is the absolute temperature. Subscript i denotes different ionic current carriers, and superscript m signifies parameters within the membrane matrix. As shown in eq 1, ion mobility and diffusivity are related through the Einstein-Smoluchowski equation, $u_i^{\mathrm{m}} = |z_i| F D_i^{\mathrm{m}}/R_{\mathrm{g}}T$.[25] To avoid potential confusion between absolute and electrical mobilities,[48] which differ by a factor of $|z_i|e$ (e is the elementary charge), diffusivity will be employed in this study to characterize ion transport within IEMs.

Mackie−Meares Model for Spatial Effect. IEMs are water-swollen polymeric films with a high density of ionic functional groups fixed to the backbone chains. The fixed moieties exclude most, but not all, like-charged co-ions, and the membrane preserves electroneutrality by having a high concentration of counterions within the matrix. Relative to the motion of ions, the polymer chains have comparatively insignificant Brownian motion and, thus, can be considered as rigid blocks.[49] Transport across IEMs can be described by the obstruction theory of diffusion,[49−51] where ions migrate through a tortuous path formed by the water phase of the membrane matrix (i.e., space occupied by the polymer is inaccessible), as illustrated in Figure 1. Based on that molecular description, the Mackie−Meares approach expresses the distribution of polymer phase using a lattice model (neglecting specific solute−membrane interactions) to yield a quantitative relationship between diffusivities within the membrane, D_i^{SE}, and in aqueous solution, D_i^{s}[49,50]

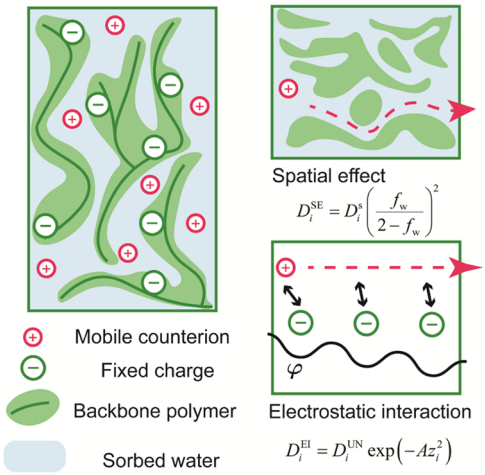

Figure 1. Schematic depicting counterion transport in a water-swollen IEM (CEM in this illustrative example), governed by spatial effect and electrostatic interaction. In the Mackie−Meares spatial model, counterions (red circles) migrate in the water phase of the membrane matrix (blue region), that is, nonobstructed, whereas the polymer phase, represented by the green region, is considered to be inaccessible for transport. The fixed functional groups, denoted by green circles, exert an attractive electrostatic force on the oppositely charged mobile counterions, retarding the ion movement. Migration of the counterion down the rough electric potential gradient, φ, causes a friction-like loss in the effective ion mobility.

https://doi.org/10.1021/acsestengg.1c00457
ACS EST Engg. 2022, 2, 1274−1286

$$D_i^{SE} = D_i^s \left(\frac{f_w}{2 - f_w} \right)^2 \quad (2)$$

where f_w is the volume fraction of water in the IEM.

The Mackie–Meares model utilizes only one parameter, f_w, which can be readily determined from the experimental measurements of membrane structural properties. This simplicity offers an advantage for transport analyses over other spatial models that require additional fitting parameters, such as the semiempirical method proposed by Yasuda,[52] $D_i^{SE} = D_i^s \exp[-B(1 - f_w)/f_w]$, with an empirical coefficient, B. The Mackie–Meares model is, hence, employed in this study. The influence of different theoretical spatial models will be further discussed in a later section.

Mobility Impediment due to Electrostatic Interaction between Mobile Counterions and Membrane Fixed Charges. In electrolyte solutions, the ions are essentially point charges that each exerts an electric field. An individual ion moving through the solution experiences these electrostatic interactions, and the net effect is a reduction in the effective mobility, particularly at high ionic strengths.[48] The classic Debye–Hückel model utilized the Poisson–Boltzmann equation to describe this phenomenon,[53] which Onsager later modified to explain molar conductivity changes at different electrolyte concentrations.[54] Previous studies, including the works of Lifson and Jackson[55−57] and Manning,[58,59] then extended the theoretical framework to polyelectrolyte solutions, where mobile counterions diffuse through charged functional groups anchored onto polymer chains in the solvent—a system highly analogous to transport in IEMs, thus providing the basis to apply the theory for the analysis of ion migration across charged membranes here.

Development of the model is detailed in the Supporting Information, and the key concepts are briefly introduced here. The phenomena of nonconvective ion transport in such fixed-charge systems can be perceived as a physics model of point charge migration down a "rough" electric potential gradient.[60] In an uncharged homogenous medium, the electric potential gradient induced by an applied external voltage is smooth. The presence of distributed fixed point charges (i.e., charged functional groups on the polymer backbone) produces an effective electric field that is the vector sum of the contribution from each point charge, resulting in a spatially nonuniform electric potential terrain. At the membrane matrix-scale, the electric field from the fixed point charges perturbs the smooth slope of the external voltage-induced potential, and the overall result is a downward sloping but "rough" electric potential (φ in Figure 1). Mobile point charges of counterions moving down the net negative gradient experience local electrostatic interactions of Coulombic attraction at nanometer length scales (typical distance between IEM fixed charges is 0.2−2 nm[42,61−63]). The roughness in the electric potential causes a friction-like loss in the macroscale effective ion mobility. Electrostatic effects from other mobile counterions in the membrane matrix will also affect transport and are factored into this model, as detailed in the Supporting Information (although these ions are not explicitly depicted in Figure 1 for simplicity in presentation). Co-ions, similarly, encounter repulsive forces from the fixed functional groups. However, because co-ion concentration within the membrane for typical IEM operations is several orders of magnitude lower than that of counterions,[42,64] the effects associated with co-ions are not considered in this analysis.

Past efforts to represent the electrostatic influence in IEMs introduced an arbitrary coefficient to adjust for the impeded ion transport. However, such empirically driven treatments are not able to reveal the underlying membrane and ion properties that govern the phenomena.[40,65] With the first-principles-based framework established by Manning as the foundation,[58] we reformulate and extend the fixed-charge lattice model to further (i) factor in membrane structural and electrical properties and (ii) account for valency of the mobile ion (detailed model derivation is presented in the Supporting Information) to yield an analytical expression to relate ion diffusivity in the rough electric potential within IEMs, D_i^{EI}, to membrane and ion properties

$$D_i^{EI} = D_i^{UN} \exp(-Az_i^2) \quad (3a)$$

$$A = \frac{\theta e^4 N_A^{2/3}}{16\pi^4 \varepsilon^2 k_B^2 T^2} c_{fix}^{m\,2/3} \quad (3b)$$

where e is the elementary charge, N_A is Avogadro constant, and k_B is Boltzmann constant. D_i^{UN} is ion diffusivity in a uniform electric field, where electrostatic interactions between ions (either mobile or fixed) can be ignored, similar to an infinitely dilute solution. Electrical properties of the IEM are reflected in parameter A of the exponential term, namely, fixed charge density (per volume of swollen membrane), c_{fix}^m, and permittivity of the membrane matrix, ε (product of vacuum permittivity and dielectric constant, $\varepsilon_0\varepsilon_r$). According to the model, the dielectric constant should describe the environment of the membrane matrix, that is, the polymer–water composite. However, as the immediate vicinity of the mobile ion is primarily water, it is plausible that the effective dielectric constant experienced by counterions is disproportionately weighed toward the water-phase dielectric constant. The point will be further addressed in the discussion sections. θ is a coefficient arising from the numerical summation of infinite vectors and is 5.48, assuming fixed functional group charges are point charges (additional assumptions and approximations are explained in the Supporting Information). Note that counter-ion-dependent swelling can affect f_w,[66] but the net effect on c_{fix}^m is marginal (≈±5% in this study). Therefore, the impact of varying membrane fixed charge density on A is insignificant, and a constant effective c_{fix}^m is used.

Integration of Spatial and Electrostatic Effects for IEM Transport Model. Combining the spatial model to account for the water and polymer phases of the IEM matrix and the electrostatic interactions between mobile ions and fixed functional groups yields an expression for the effective ion mobility within the membrane

$$D_i^m = D_i^s \left(\frac{f_w}{2 - f_w} \right)^2 \exp(-Az_i^2) \quad (4a)$$

A logarithmic transformation linearizes the relationship between the logarithm of the diffusivity ratio, $\ln(D_i^m/D_i^s)$, and the ion valency squared, z_i^2, with a negative slope of A and the natural logarithm of the Mackie–Meares spatial parameter, $2\ln[f_w/(2 - f_w)]$, being the intercept

$$\ln\left(\frac{D_i^m}{D_i^s}\right) = -Az_i^2 + 2\ln\left(\frac{f_w}{2 - f_w}\right) \quad (4b)$$

https://doi.org/10.1021/acsestengg.1c00457
ACS EST Engg. 2022, 2, 1274−1286

Equation 4b enables regression analyses on the transport model, specifically, to quantitatively evaluate the roles of ion valency and membrane structural and electrical properties of water volume fraction, fixed charge density, and dielectric constant on ion migration.

MATERIALS AND METHODS

Membranes and Chemicals. Three commercial CEMs, Selemion CMV (Asahi Glass, Tokyo, Japan), Fumasep FKS-50 (FUMATECH BWT GmbH, Bietigheim-Bissingen, Germany), and MEGA Ralex CMHPES (MEGA a.s., Straz pod Ralskem, Czechia), and one AEM, Selemion AMV (Asahi Glass, Tokyo, Japan), were procured from the manufacturers. The charged functional groups of the CEMs and AEM are sulfonate and quaternary ammonium, respectively.[67−72] Fumasep FKS is a homogeneous membrane, whereas the other three are composite membranes containing support layers.[67−72] Salts and salt hydrates of NaCl, $CaCl_2{\cdot}2H_2O$, $MgCl_2{\cdot}6H_2O$, $AlCl_3{\cdot}6H_2O$, $LaCl_3{\cdot}7H_2O$, Na_2CO_3, and $Na_3PO_4{\cdot}12H_2O$ were acquired from Alfa Aesar (Ward Hill, MA). NaBr, $NaNO_3$, and Na_2SO_4 were obtained from ACROS Organics (Morris Plains, NJ), whereas KCl was acquired from LabChem (Zelienople, PA). All chemicals were ACS or higher grade and used as received to prepare the electrolyte solutions for counterion diffusivity experiments. Deionized (DI) water was obtained from a Milli-Q ultrapure water purification system (Millipore, Billerica, MA).

Structural Properties Characterization. Three membrane structural properties of ion-exchange capacity, swelling degree (SD), and polymer density were characterized to investigate the transport mechanisms governing counterion mobility. Ion-exchange capacity, IEC, is defined as the number of fixed charges per unit weight of the dry membrane.[11] The IECs of CEMs were determined using the acid titration method,[73,74] while the AEM was characterized by the ion elution method.[75,76] SD is defined as the mass of sorbed water per unit mass of the dry polymer.[11] Because membrane swelling is affected by the counterion in the membrane matrix,[66] the membranes were soaked in the same electrolyte solutions as the conductivity measurement experiments (1.0 equiv/L). For each IEM, SDs for different counterions were calculated from the wet and dry masses of the membranes,[73] correcting for the contribution from sorbed counterions. Polymer densities of the dry membranes, ρ_p, were characterized with a pycnometer using DI water.[77] Detailed characterization protocols for IEC, SD, and ρ_p can be found in the Supporting Information. Volume fraction of water, f_w, describes the available volume within the IEM matrix for ion transport and is calculated as[64]

$$f_w = \frac{SD/\rho_w}{SD/\rho_w + 1/\rho_p} \quad (5)$$

where ρ_w is the volumetric mass density of water. The number of fixed charges per unit volume of the wetted membrane is the IEM fixed charge density, c_{fix}^m[64]

$$c_{fix}^m = IEC\frac{\rho_w f_w}{SD} \quad (6)$$

Electrochemical Properties Characterization. Diffusivities of different counterions in each membrane were characterized using direct current chronopotentiometry in a four-electrode cell with an electrochemical workstation (Interface 1010E, Gamry, Warminster, PA).[73] Counterions investigated for the three CEMs are Na^+, K^+, Mg^{2+}, Ca^{2+}, Al^{3+}, and La^{3+}, whereas Cl^-, Br^-, NO_3^-, CO_3^{2-}, SO_4^{2-}, and PO_4^{3-} were examined for the AEM. Co-ions for the CEMs and AEM are Cl^- and Na^+, respectively. Single electrolyte solutions at 1.0 equiv/L were prepared for the diffusivity measurements (e.g., 1.0 M NaCl, 0.50 M Na_2SO_4, and 0.33 M $AlCl_3$ for mono-, di-, and trivalent counterions, respectively). The intermediate concentration of 1.0 equiv/L was purposefully chosen to minimize the interference of boundary layer resistance at lower concentrations.[78] Before the electrochemical characterizations, the membranes were soaked in the electrolyte test solution for more than 24 h. Transport numbers of the counterions were utilized to exclude the current contribution from co-ions. Dielectric permittivity properties of hydrated IEMs were characterized by dielectric relaxation spectroscopy, DRS, in the microwave frequency range on a vector network analyzer (VNA, N9928A, Keysight, Santa Rosa, CA).[79−81] Detailed procedures of the electrochemical measurements and related considerations can be found in the Supporting Information.

RESULTS AND DISCUSSION

"Valency Gap" in Counterion Mobility. Figure 2 shows the experimentally determined diffusivities of Na^+, K^+, Mg^{2+}, Ca^{2+}, Al^{3+}, and La^{3+} counterions in Selemion CMV CEM (columns) and literature values of ion diffusivities in an infinitely diluted aqueous solution (symbols).[82] All counterion diffusivity results for the IEMs are listed in Tables S4−S7 of the Supporting Information. In bulk solution, ions with the same valency have similar diffusion coefficients (within 32%) despite the disparate molecular weights. However, the diffusivities are significantly lower as the charge on the ion increases: D_i^s reduces by 54−72% as ion valency rises from +1 to +3. These D_i^s trends are primarily governed by the size of the hydrated ion in bulk aqueous medium.[48] Despite the difference in bare radius, ions of the same valency end up with comparable hydrated sizes, whereas a higher charge produces greater ion-dipole attraction forces, resulting in more solvating water molecules and, hence, a larger hydrated ion size with correspondingly lower diffusivity.

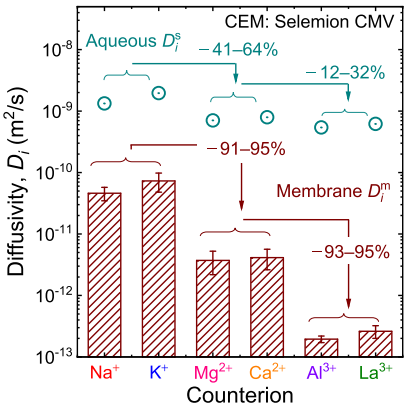

Figure 2. Diffusivities of different mono-, di-, and trivalent counterions in Selemion CMV CEM, D_i^m (columns), and bulk aqueous solution, D_i^s (symbols, data from literature).[82] Percentages indicate the decrease in diffusivity from mono- to divalent ions and di- to trivalent ions.

The counterion diffusivities in the membrane matrix are at least 1 order of magnitude lower than the aqueous diffusivities

https://doi.org/10.1021/acsestengg.1c00457
ACS EST Engg. 2022, 2, 1274−1286

($<10^{-10}$ m^2/s compared to $\approx 10^{-9}$ m^2/s). The diminished mobility of ions within the IEM is expected, given the reduced availability of nonobstructed volume for transport. Similar to the behavior in bulk solution, ions of the same valency have comparable D_i^m. More importantly, D_i^m between ions of different valencies drops much more drastically (approximately one order of magnitude) when contrasted against the aqueous solution trend. This markedly greater decline in ion mobility in the IEM cannot be explained by the ion hydration size.

The trend exhibited in Figure 2, which we term the "valency gap" of counterion mobility, is commonly observed in IEM studies.[29,39,40,83] Although different counterions can induce varying degrees of membrane swelling,[66] which in turn affects the volume fraction of water, f_w (eq 5), SD alone is not sufficient to cause the order of magnitude discrepancy (SD data are presented in Tables S2 and S3 of the Supporting Information and membrane ρ_p and IEC are summarized in Table S1), as pointed out by previous studies.[29,40,66] Critically, the scale of the gap deviates between different membranes (factor of 83−950 for the three CEMs), strongly suggesting that the underlying mechanisms are influenced by membrane properties. The diffusivity data indicate that counterion mobility within IEMs is influenced by a charge-dependent effect; we hypothesize that the underlying mechanism is the electrostatic interaction between mobile counterions and fixed charges of the IEM, that is, higher valency ions experience greater retardation due to stronger electrostatic attractions.

Regression Analyses on Counterion Diffusivity Show Good Agreement with the Transport Model for CEMs. Regression analyses were carried out on the diffusivities of the six counterions using the model described by eq 4b for the three commercial CEMs. Figure 3 presents the linear regression of the logarithmic reduction of membrane diffusivity compared to aqueous diffusivity, $\ln(D_i^m/D_i^s)$, on the ion valency squared, z_i^2 (i.e., 1^2, 2^2, and 3^2). The regression results are summarized in Table 1.

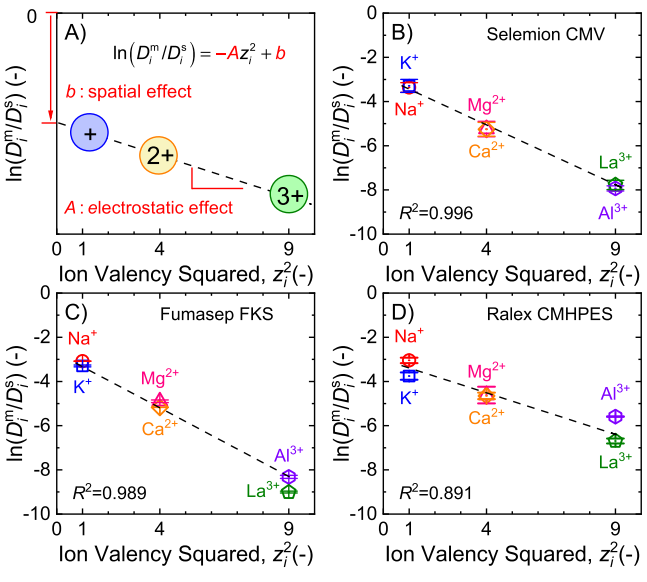

Figure 3. Regression analyses on counterion diffusivities in CEMs: (A) Illustrative plot depicting electrostatic and spatial effects of the model. (B) Selemion CMV, (C) Fumasep FKS, and (D) Ralex CMHPES. The natural logarithms of membrane diffusivity over aqueous diffusivity, $\ln(D_i^m/D_i^s)$, are regressed on the ion valency squared, z_i^2, of the counterions. The vertical axis intercept, b, is determined by the spatial effect, while the slope, A, describes the strength of the electrostatic effect.

The transport model presented earlier indicates a linear dependence of $\ln(D_i^m/D_i^s)$ on z_i^2, with the electrostatic effect represented by the slope of the fitting line and the vertical axis intercept denoting the spatial effect (Figure 3A and eq 4b). The regressions yielded excellent fits for Selemion CMV and Fumasep FKS CEMs, with coefficients of determination, R^2, of 0.996 and 0.989. A good fit was also obtained for Ralex CMHPES, with R^2 = 0.891. Using the intercept values, b, the volume fraction of water, f_w, was back-calculated with eq 4b, that is, Mackie−Meares model, to be 38.6, 46.0, and 34.3% for Selemion CMV, Fumasep FKS, and Ralex CMHPES, respectively, which falls within the reasonable range for common IEMs.[13,42,64] We further note that the back-calculated f_w of Ralex CMHPES is relatively close to the reported experimental measurements, but the other two membranes have larger deviations from literature values. Further analyses of the volume fraction of water and membrane swelling are discussed in the next sections. The generally consistent agreements between experimental diffusivity data and membrane structural property (i.e., f_w) with theoretical calculations provide substantiation for the model presented in this study, that is, ion transport in IEMs; specifically, the valency gap can be described by the primary mechanisms of spatial effect and electrostatic interaction. The next sections further examine the quantitative relationships between counterion mobility and membrane properties in the context of the two phenomena.

Spatial Effect Is Better Modeled by Accounting for Counterion-Dependent Membrane Swelling. The Mackie−Meares spatial model is governed by the volume fraction of water, f_w (eq 2), which is in turn determined by the membrane SD (eq 5). Because different counterions swell the membrane to varying degrees,[66] the water uptakes of IEMs in each 1.0 equiv/L electrolyte solution were measured to investigate the effect of swelling. Figure 4A presents the SD of Ralex CMHPES with the six counterions (symbols, left vertical axis), and the data of other membranes are listed in Table S2 of the Supporting Information. SD generally declines as the valency increases, dropping from 0.465 (Na^+) to 0.388 (La^{3+}), with the exception of K^+. The negative correlation between water uptake and valency is due to the change in the swelling pressure. Raising the valency from 1 to 2 and 3 reduces the total number of counterions in the membrane matrix to 1/2 and 1/3, respectively, consequently lowering the swelling pressure difference across the aqueous−membrane interface and, thus, lessening the water uptake.[66] The lower swelling of K^+ was also commonly observed in ion-exchange polymer studies and can be attributed to the substantially lower hydration energy of the ion.[66,84,85] The other two CEMs exhibited similar trends (Table S2 of the Supporting Information).

The experimentally characterized SDs can be used to calculate the volume fractions of water, f_w, with eq 5, which were then utilized to determine the Mackie−Meares spatial parameters, $[f_w/(2 - f_w)]^2$, that is, intercept in eq 4b. The results are shown in Figure 4A (columns, right vertical axis). Because of the range of SDs induced by the different counterions, $[f_w/(2 - f_w)]^2$ varies between 0.0301 and 0.0458 for the Ralex CMHPES CEM, that is, changes to the structure of the membrane matrix influenced the counterion mobility by altering the volume available for ion migration. Swelling elasticity of the membranes is accounted for by

https://doi.org/10.1021/acsestengg.1c00457
ACS EST Engg. 2022, 2, 1274−1286

Table 1. Fitting Parameters of the Regression Analyses, Coefficient of Determination (R^2), Slope (A), Vertical Axis Intercept (b), Effective Dielectric Constant (ε_r), before and after SD Correction, Experimentally Determined Fixed Charge Density (Averaged across the Six Counterions), c_{fix}^m, and Dielectric Constant Measured by DRS, ε_{DRS}, of the Three Commercial CEMs

		Selemion CMV	Fumasep FKS	Ralex CMHPES
	c_{fix}^m (M)	2.23	1.69	1.72
initial fitting (without SD correction)	R^2	0.996	0.989	0.891
	slope, A	0.561	0.688	0.339
	intercept, b	−2.86	−2.42	−3.14
	effective dielectric constant, ε_r	62	51	73
after SD correction	R^2	0.986	0.985	0.907
	slope, A	0.540	0.691	0.329
	intercept, b^*	0.823	1.73	0.103
	effective dielectric constant, ε_r	63	51	74
DRS measurement	delectric constant, ε_{DRS}	3.7 ± 0.3	3.2 ± 0.2	7.7 ± 0.9

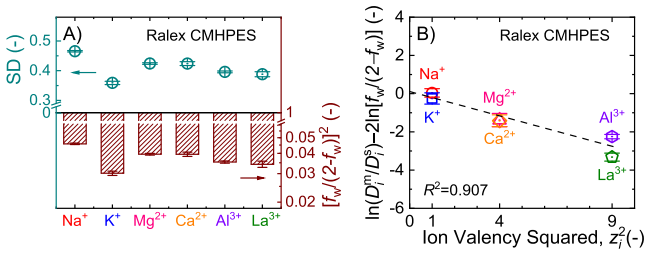

Figure 4. Influence of counterion-dependent swelling on the spatial effect and membrane counterion diffusivities: (A) SD (symbols, left vertical axis) and the Mackie−Meares spatial parameter, $[f_w/(2 - f_w)]^2$ (columns, right vertical axis), for different counterions; (B) regression analysis of counterion mobilities on the ion valency squared, z_i^2, accounting for different membrane swelling by subtracting the natural logarithms of the Mackie−Meares spatial parameter from the diffusivity ratio between membrane and bulk solution, $\ln(D_i^m/D_i^s) - 2\ln[f_w/(2 - f_w)]$. The vertical axis intercept is defined as the fitting residual, b^*, and the slope of the regression line, A, describes the strength of the electrostatic effect. Only Ralex CMHPES CEM is presented for brevity and concision; results for other IEMs are shown in Table S2 of the Supporting Information.

incorporating the natural logarithm of the Mackie−Meares spatial parameter into the regression analysis

$$\ln\left(\frac{D_i^m}{D_i^s}\right) - 2\ln\left(\frac{f_w}{2 - f_w}\right) = -Az_i^2 + b^* \quad (7)$$

where b^* is defined as the model fitting residual (discussed later). The SD-corrected regression for Ralex CMHPES is shown in Figure 4B, and the fitting parameters for the three CEMs are reported in Table 1. Accounting for counterion-dependent membrane swelling improved the R^2 of Ralex CMHPES from 0.891 to 0.907. Excellent fittings were still obtained for the other two membranes, although R^2 marginally decreased to 0.986 and 0.985. Additionally, the strength of electrostatic interactions, that is, the slope of regression lines, did not change significantly after the SD correction and is analyzed next.

Electrostatic Interaction of Charged Membrane Matrix on Counterions Retards Migration. In the proposed transport model, the electrostatic interaction between mobile counterions and fixed charged groups of the membrane matrix is represented by the slope of the regression line, A, and is expressed as a function of fixed charge density, c_{fix}^m, and effective dielectric constant, ε_r, of the IEM; specifically, $A \propto c_{fix}^{m2/3}$, ε_r^{-2} (eq 3b). Therefore, counterion mobility is quantitatively related to the structural and electrical properties of the membranes. Table 1 lists the average fixed charge density determined from ion-exchange capacity measurements and different SDs induced by the six counterions (eq 6). Using experimentally characterized c_{fix}^m and model regression parameter A, the remaining unknown of effective dielectric constants are determined to be 63, 51, and 74 for Selemion CMV, Fumasep FKS, and Ralex CMHPES, respectively (Table 1). All three values lie between the dielectric constants of pure water at ambient conditions (≈78)[86] and the unhydrated polymers of common IEMs (<10).[19,87−89] As the membrane matrix is a composition of the water and polymer phases, the dielectric constant experienced by mobile counterions migrating across the IEM can be expected to be a function of the composition and dielectric constants of water and polymer.[88] More hydrated IEMs would, hence, exhibit permittivity closer to water. The experimentally determined f_w values match this expected trend, with membranes of higher water volume fraction (Ralex CMHPES > Selemion CMV > Fumasep FKS) showing greater ε_r. Because the electrostatic interaction is inversely proportional to the square of the dielectric constant, a lower ε_r indicates a membrane with a stronger electrostatic interaction.[90] Therefore, a membrane with higher water content has a weaker valency-dependent electrostatic effect.

Experimental characterization of the bulk membrane permittivity using dielectric relaxation spectroscopy gave a consistent ε−f_w trend. The static relative permittivity at the high-frequency range yielded dielectric constants of 3.7, 3.2, and 7.7 for hydrated Selemion CMV, Fumasep FKS, and Ralex CMHPES, respectively (Table 1). These experimental measurements rank in the same order as ε_r determined from regression analyses of the transport model, thus offering additional support that membranes with greater water content experience weaker electrostatic effect. We note that the absolute values of membrane dielectric constants characterized by DRS are much lower than the model-derived ε_r values. The DRS measurements are closer to the range of polymer-only dielectric constants,[19,87−89] whereas the model-derived results are more similar to pore water.[91] We postulate that the discrepancy is possibly attributed to two factors: DRS inherently characterizes global (or bulk average) dielectric

https://doi.org/10.1021/acsestengg.1c00457
ACS EST Engg. 2022, 2, 1274−1286

properties and the model potentially overestimating electrostatic interactions.

DRS measures the bulk relative permittivity of hydrated membranes, and hence, measurements include contributions from both water and polymer components of the IEMs. As the continuous phase of the polymer is a significantly greater portion of the hydrated IEM than the dispersed phase of water, measurement of the bulk dielectric constant is nearer to the polymer property.[87,88] However, at the molecular scale, the space for electrostatic interactions between the mobile counterion and the closest fixed functional groups is mostly water-filled. Therefore, the effective dielectric constant experienced by the migrating ion should be principally governed by the local dielectric environment, that is, primarily water in the nonpolymer phase of the membrane, rather than the bulk average relative permittivity. However, nanoscale dielectric environment within IEMs is not experimentally accessible at present. In the Supporting Information, the Maxwell−Garnett approach for effective medium approximation is employed to show that the dielectric constant of the water phase in the membrane, ε_w, may match the ε_r values from the model. However, actual calculations of ε_w using the Maxwell−Garnett method require highly precise measurements of both the dry membrane dielectric constant and the fractional water volume that are beyond the limits of current characterization techniques.

Another possible reason for the mismatch between DRS-characterized and model-derived ε_r may be due to incompleteness of the proposed transport framework in describing the actual electrostatic effect. The model simplifies the electrostatic forces between fixed functional groups and mobile counterions to be point charge interactions. In reality, the two charged entities have finite volumes and are not point charges (e.g., bare and hydrated radii of the mobile ions range from 0.50−1.15 and 3.31−4.75 Å,[92] respectively). Thus, in the nanoscale space of the membrane matrix, the simplifying assumption of point charge interactions may not always hold true. The model, hence, likely overestimates the electrostatic interactions, leading to a higher dielectric constant back-calculated from the fitting parameter, A.

The model fitting residual, b^*, represents the general validity of the proposed transport model and unavoidable experimental variations. Ideally, the fitting lines based on eq 7 should pass through the origin, that is, $b^* = 0$. The model fitting residual of 0.103 for Ralex CMHPES is close to this ideal, but the residual intercepts of Selemion CMV and Fumasep FKS are significantly greater than zero at 0.823 and 1.73, respectively (Table 1 and Figure 4B), that is, the model underestimates experimental ion diffusivities. The deviations can be caused by uncertainties in the experimental measurements, the interference of the enmeshed support layer, and imprecisions of the models in describing the complete transport phenomena. Inevitable random errors in the experimental measurements, mainly characterization of the ionic conductivity[93] and gravimetric measurements of water volume fraction in the membranes,[94] may have contributed to the nonzero b^*. Commercial IEMs commonly possess an enmeshed support layer (the Fumasep FKS membrane in this study is an exception),[95] which can potentially influence transport, for example, by decreasing the available volume for ion permeation and increasing tortuosity of the transport pathway. Such factors are not explicitly considered in the current approach. In the electrostatic interaction and spatial effect models, the simplifying assumptions necessary to express ion transport down a rough electric potential gradient and across tortuous paths of nonobstructed volume as analytical expressions, eqs 3a, 3b, 4a, and 4b, likely promoted variances in the estimated diffusivity. Additionally, neglecting the finite volume of the charged entities, as discussed above, possibly tilted the regression line slopes and resulted in a fitting residual, whereas the decreased accuracy of the Mackie−Meares model for low SD membranes can also lead to divergence from the actual D_i^{SE}.[49,50] The Yasuda model, an alternative semiempirical approach to quantify the spatial effect, assumes the effective free volume to be proportional to the water volume, which introduces a empirical factor, B, to yield $D_i^m = D_i^s \exp[-B(1 - f_w)/f_w]$.[52] The additional empirical factor affords greater flexibility to account for other effects, such as membrane microstructure, hydrodynamics, and specific solute features,[51] to enhance the precision of model predictions.

Weaker Electrostatic Effect Observed in AEMs. Figure 5A presents $\ln(D_i^m/D_i^s)$ as a function of z_i^2 for AEM Selemion

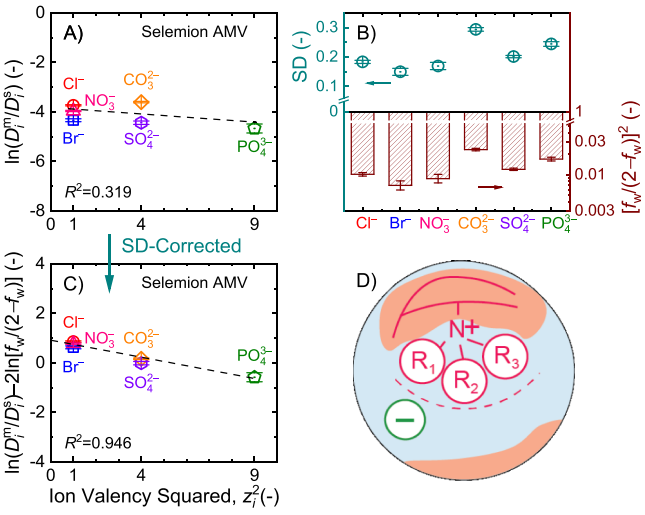

Figure 5. Analyses on counterion diffusivities in the AEM, Selemion AMV: (A) Logarithms of membrane diffusivity over aqueous diffusivity, $\ln(D_i^m/D_i^s)$, regressed on the ion valency squared, z_i^2, of the counterions; (B) SD (symbols, left vertical axis) and the Mackie−Meares spatial parameter, $[f_w/(2 - f_w)]^2$ (columns, right vertical axis), for different counterions; (C) SD-corrected regression incorporating the Mackie−Meares spatial parameter. (D) Schematic illustrating hydrocarbon groups, $R_{1,2,3}$, sterically hindering the mobile anion from approaching the charged nitrogen atom (N^+), thus weakening the electrostatic interaction.

AMV. Compared to CEMs (Figure 3B−D and Table 1), the drop in diffusivity as valency increases is not as pronounced. The regression analysis of ion diffusivity on valency, without SD corrections, is also shown. The poor fitting, with a low R^2 of 0.319, is due to the water uptake behavior of the AEM with different anions. Unlike the CEMs, which have a considerably narrower range of SDs across the different cations (relative variability within 11%), the SD of the AEM varied more drastically across the anions investigated (relative variability of 23.5%). Additionally, multivalent anions, especially CO_3^{2-} and PO_4^{3-}, produced significantly higher water uptake in Selemion AMV than monovalent species (Figure 5B), opposite to the observed trend for CEMs. As expected, accounting for the swelling elasticity with eq 7 yielded greatly improved fitting (R^2

https://doi.org/10.1021/acsestengg.1c00457
ACS EST Engg. 2022, 2, 1274−1286

= 0.946, Figure 5C). Detailed SD results are reported in Table S3 of the Supporting Information, along with discussion on the treatment for phosphate ions.

The strength of the electrostatic effect, signified by the regression line slope after the SD-correction, is appreciably lower for the AEM than those for the CEMs (0.172 and 0.329−0.691, respectively). The weaker electrostatic interactions can be attributed to the molecular structure of quaternary ammonium, the typical fixed charge group in the AEMs.[11,13] As discussed previously, Coulombic attraction forces are determined by the distance between the two charges. The four hydrocarbon groups in quaternary ammoniums can sterically hinder mobile anions from approaching the positively charged nitrogen atom (Figure 5D),[96] thereby limiting the attractive interactions and weakening the overall electrostatic effect. The sterically obstructed electrostatic interaction is a plausible explanation for the effective dielectric constant of 105 calculated from the point charge-based model, which is even larger than that of pure water (≈78). The weakening of electrostatic interaction by steric obstruction has been reported to affect sorption selectivity in ion-exchange studies.[66,97,98] In contrast, the sulfonate functional group of the CEMs does not experience such steric hindrance.

Relation of Spatial Effect and Electrostatic Interaction to Other Models and Theories. Previous models and theories have been put forth to describe the general ion transport in IEMs and, more specifically, explain the relationships between ion mobility and properties of the membrane and ion.[21,31,41,44,99−103] This section discusses the relations and principal differences between some of the prevailing approaches and the current proposed framework. The hydration energy of mobile ions has been reported to negatively correlate with ion conductivity or permeability in IEMs.[41,104] Hydration energy can influence ion transport in IEMs through several mechanisms, including ion partitioning across the solution−membrane interface,[104] alteration of ion transport pathway due to changes in membrane SD,[66] influence of hydrated ion size on mobility,[48,66] and ion−water interactions within the IEM.[41] Although ion hydration−dehydration at the interface can influence the partitioning of the species into the membrane matrix,[104,105] it is unlikely to change diffusivity, which is the mobility of ions in the IEM. Hydration energies of different ions affect membrane SD and determine the Stokes radii.[48,66] The impacts of these two phenomena of pathway alteration and hydrated ion size on ion transport are expressed in the Mackie−Meares spatial parameter (through the fractional volume of water, f_w) and reflected in the bulk phase aqueous diffusivity, respectively. However, as discussed earlier, the mechanisms by themselves are insufficient to quantitatively explain the orders of magnitude gap in counterion mobility observed in Figures 2−5. Furthermore, a recent study on polyamide membranes suggests that sodium ions in large channels with radii > 0.5 nm exhibit no observable difference in average hydration number compared to the bulk solution.[106] IEMs have substantially greater SDs than the dense polyamide membranes and also have more open architectures (for instance, Nafion membranes possess water clusters with radii of 2−2.5 nm connected by channels of 0.5−0.75 nm radii).[61] Therefore, the role of hydration is unlikely to be significant.

A past study conjectured that ions permeating across the IEM continually associate and disassociate with water molecules in the membrane matrix.[41] Ions of higher valence have larger absolute values of hydration energy and would, therefore, experience higher energy barriers during transport. Di- and trivalent ions are, thus, more hindered.[99] It is doubtful that the phenomenon, if indeed it occurs, is the dominant mechanism and can fully account for the valency gap. Ion-dipole forces between counterions and water are significantly weaker than ion−ion attraction between charged mobile ions and fixed functional groups. Therefore, it is more plausible that electrostatic interaction is the primary mechanism governing counterion transport. The observed correlation between ion transport and hydration energy reported by the past study[41] can be alternatively explained by the underpinning factor of ion valency, which influences hydration energy (ions with higher valency have greater absolute values of hydration energy)[99] but also plays a central role in the electrostatic effect presented here. Findings of a recent work offer further support for the proposed electrostatic interaction model.[100] The study combined quantum chemistry calculations and experimental measurements to quantitatively show that electrostatic interaction is the dominant effect for counterions with different charges.

The counterion condensation theory,[59] which was recently applied to predict activity coefficient, diffusivity, and salt permeability of ions in IEMs,[42−44,107] also considered the effects of rough electric potential on ion migration. The counterion condensation model, however, has a principal difference that distinguishes it from the approach presented in this current study. Under the counterion condensation framework for self-diffusion, a fraction of the mobile counterions is considered to be associated with the membrane fixed charges, that is, condensed, with the remainder counterions being uncondensed. The condensed counterions are treated as immobile point charges and have a shielding effect on the electric field exerted by the fixed charges. Hence, although the uncondensed counterions experience impeded transport due to the rough electric potential, the effect is lessened because of the shielding of the electric field by the condensed counterions. In contrast, the model presented here does not discretize the condensation state of the counterions, and therefore, all mobile counterions are exposed to the undiminished rough electric potential.

In the counterion condensation model, quantification of counterion mobility requires detailed information of micro- and nanoscale structural and material properties, especially when assessing the condensed phase mobility in low SD membranes.[43,44,62,107] In contrast, the approach presented in this study does not segregate the counterions into condensed and uncondensed phases to apply separate treatments because the spatial effect and electrostatic interaction are described using macroscale parameters. As such, the model parameters, c_{fix}^{m}, ε, f_w, z, and D, are more experimentally accessible, enabling the framework presented in this study to quantitatively assess the governing phenomena in IEM transport and elucidate the roles of membrane and ion properties. Importantly, a recent study reported that condensed counterions actually contribute significantly to net ion transport under an electrochemical potential gradient.[44] This finding is at odds with the original assumption of the counterion condensation model, which specifies that condensed ions are immobile, and highlights the need to further modify the theoretical framework in order to develop quantitative relationships for the condensed phase. Nonetheless, we note that the counterion condensation model and this approach are not mutually exclusive; the two

https://doi.org/10.1021/acsestengg.1c00457
ACS EST Engg. 2022, 2, 1274−1286

frameworks can potentially be merged into a unified theory for transport in IEMs.

The electrostatic effect model described by eq 3b of the main manuscript quantifies the influence of fixed charge density, c_{fix}^{m}, and temperature, T. In the model, the electrostatic effect parameter, A, is a function of c_{fix}^{m} and T by power-law relations with exponents of 2/3 and −2, respectively, that is, $A \propto c_{fix}^{m2/3}$, T^{-2}. Onsager examined electrolyte solution systems where both cations and anions are mobile and derived a corresponding relationship, which indicates that the normalized diffusivity drop is proportional to the square root of concentration, that is, $\Delta D/D \propto c^{1/2}$.[54] The relationship has been adopted to describe the electrostatic interactions between charged entities inside IEMs[31] (the distinctions between Onsager's approach from the framework used by the model presented here were discussed in another study).[58] However, Onsager's relationship is based on a system with both positively and negatively charged entities being mobile and, hence, does not correctly describe the physics of transport in IEMs, where only counterions are mobile and charged functional groups are stationary. Because of this principal conceptual difference, Onsager's relationship, therefore, is expected to underestimate the retarding effect of electrostatic interactions in IEMs. The $A \propto c_{fix}^{m2/3}$ relationship of the electrostatic interaction model presented here is, hence, mechanistically more rigorous.

Several IEM studies adopted an activated diffusion model to describe ion movement, expressing diffusivity with the Arrhenius equation, $D_i = D_i^{o} \exp(-E_a/R_gT)$.[100,101,104] E_a is the activation energy and describes the energy barriers including, but not limited to, electrostatic effects.[100] The power-law exponent of T in the Arrhenius equation is −1, and previous regression analyses of ion diffusivities at different temperatures produced reasonably good fittings.[100,101] This finding appears to contradict the validity of the electrostatic interaction model (eq 3b), which specifies a power-law exponent of −2. However, closer scrutiny of the temperatures used in the regressions reveals a significant shortcoming in the past analyses. Because the water-swollen IEMs operate over a relatively narrow range of ≈0−40 °C (273−313 K), regression analyses are inherently not able to definitively differentiate the power-law exponent of T (e.g., T^{-1} varies by < 13% in the investigated range).[58] As such, the quantitative influence of temperature on ion transport in IEMs is yet to be conclusively determined.

IMPLICATIONS

A more complete understanding of the structure−property performance relationships of IEM transport can inform the advancement of ion-selective separations. In this study, we present a first-principles-based model with two governing phenomena, the spatial effect of sorbed water and the electrostatic interactions between mobile ions and fixed charges, to describe counterion mobility in membranes. Application of the theoretical framework to analyze the experimental results showed that the orders-of-magnitude gaps between membrane mobilities of counterions with different valencies can be attributed to the retarding effect of electrostatic interaction. Importantly, the model quantitatively relates counterion diffusivity to experimentally accessible membrane properties of fractional water volume, fixed charge density, and dielectric constant.

The transport model presented here demonstrated good agreement with experimental measurements but is by no means a complete description of the transport phenomena in IEMs. To further improve the framework and potentially achieve predictive uses, subsequent research efforts can probe the local dielectric property and steric hindrance between mobile ions and fixed charge groups and improve the rigor of the spatial effect of available volume for ion transport. Other frictional effects, such as molecular frictions of the mobile ion with other mobile ions and with the backbone polymers, are not considered in this study but can also exert significant influence on the ion mobility.[45] In addition, specific ion effects, such as ion pairing,[108,109] formation of ionic condensates,[103] and chelation,[22] may play a role in counterion mobility but are not explicitly included in this model. These ion-specific interactions could possibly explain the discrepancies between ions with the same valency or contribute to the fitting residuals (Figures 3−5). The formulation of a comprehensive and robust transport model based on fundamental understanding of the underlying mechanisms can further elucidate the governing structure−property performance relationships.

The findings of this study have significant implications for selective ion separations that are environmentally relevant. For separations that require the discrimination of ion valencies, for example, segregating mono- and divalent ions in water softening and heavy metal (Pb^{2+}, Hg^{2+}, Cd^{2+}, and Cr^{2+}) removal, the ion mobility model indicates that stronger electrostatic interactions between the counterions and fixed charges would yield greater differentiation between the membrane diffusivity of counterions with different valencies. Thus, membranes with lower water uptake, higher charge density, and smaller dielectric constant are required to enhance valency-based selectivity. However, overall ion transport is the combination of ion sorption into the membrane, followed by electromigration or diffusion across the IEM.[11] Net selectivity is, therefore, the combination of sorption selectivity and diffusion selectivity (affinity and mobility, respectively). As stronger electrostatic interactions would favor the sorption of higher valency counterions,[66] a tradeoff between affinity and mobility potentially exists, which would need to be considered in the design of valency-selective separations and IEMs. IEMs coated with oppositely charged thin layers or multilayers of alternating charge can achieve improved valency selectivity through greater electrostatic repulsion of multivalent ions than monovalent ions,[110,111] that is, a different mechanism from the electrostatic interaction examined here, but the selectivity enhancement is obtained at the expense of diminished permeation fluxes, analogous to the conductivity-permselectivity tradeoff.[64]

An even more challenging separation task is the selective transport of specific counterions from others with the same valency. Examples of such applications include harvesting lithium from produced water, recovering nitrogenous nutrients from waste streams, and removal of environmentally relevant oxyanions (e.g., $H_2AsO_4^-$, $H_2BO_3^-$, and $H_2PO_4^-$) from Cl^- and HCO_3^- background ions.[1−3,21,22] The current transport framework suggests that the spatial effect and electrostatic interaction are unable to adequately discern between counterions with identical valencies. Therefore, phenomena beyond those in the present transport model, such as ion-specific effects, would need to be engineered into the separation process and membrane development to realize such high-precision transport selectivity.

https://doi.org/10.1021/acsestengg.1c00457
ACS EST Engg. 2022, 2, 1274−1286

■ ASSOCIATED CONTENT

Supporting Information

The Supporting Information is available free of charge at https://pubs.acs.org/doi/10.1021/acsestengg.1c00457.

Derivation of the analytical equation for electrostatic effect; detailed experimental methods and relevant considerations on the characterization of ion-exchange capacity, SD, polymer density, membrane conductivity and diffusivity, transport number, and dielectric permittivity; polymer density, ion-exchange capacity, and SD of the membranes; diffusivities of different counterions in the membranes; and discussions on dielectric constants of the hydrated membranes (PDF)

■ AUTHOR INFORMATION

Corresponding Author

Ngai Yin Yip − *Department of Earth and Environmental Engineering and Columbia Water Center, Columbia University, New York, New York 10027-6623, United States;* orcid.org/0000-0002-1986-4189; Phone: +1 212 8542984; Email: n.y.yip@columbia.edu

Authors

Hanqing Fan − *Department of Earth and Environmental Engineering, Columbia University, New York, New York 10027-6623, United States*

Yuxuan Huang − *Department of Earth and Environmental Engineering, Columbia University, New York, New York 10027-6623, United States*

Ian H. Billinge − *Department of Earth and Environmental Engineering, Columbia University, New York, New York 10027-6623, United States*

Sean M. Bannon − *Department of Chemical Engineering, University of Virginia, Charlottesville, Virginia 22904, United States*

Geoffrey M. Geise − *Department of Chemical Engineering, University of Virginia, Charlottesville, Virginia 22904, United States;* orcid.org/0000-0002-5439-272X

Complete contact information is available at: https://pubs.acs.org/10.1021/acsestengg.1c00457

Notes

The authors declare no competing financial interest.

■ ACKNOWLEDGMENTS

G.M.G. and S.M.B.: Acknowledgment is made to the Donors of the American Chemical Society Petroleum Research Fund for partial support of this research. We thank the anonymous reviewers for their critical reading of the manuscript and suggestions to improve the analysis.

■ REFERENCES

(1) National Academies of Sciences, Engineering, and Medicine. *A Research Agenda for Transforming Separation Science*; The National Academies Press: Washington, DC, 2019.

(2) Tirrell, M.; Hubbard, S.; Sholl, D.; Peterson, E.; Tsapatsis, M.; Maher, K.; Tumas, W.; Giammar, D.; Gilbert, B.; Loo, Y.-L.; Schoonen, M.; Kung, H.; Garrett, B.; Horton, L.; McLean, G.; Darling, S.; Runkles, K. *Basic Research Needs for Energy and Water: Report of the Office of Basic Energy Sciences Basic Research Needs Workshop for Energy and Water*; USDOE Office of Science (SC) (United States), 2017.

(3) Clark, S. B.; Buchanan, M. V.; Wilmarth, B. *Basic Research Needs for Environmental Management*; Pacific Northwest National Lab. (PNNL): Richland, WA (United States), 2016.

(4) Li, W.-W.; Yu, H.-Q.; Rittmann, B. E. Chemistry: Reuse Water Pollutants. *Nature* **2015**, *528*, 29−31.

(5) Ye, Y.; Ngo, H. H.; Guo, W.; Chang, S. W.; Nguyen, D. D.; Zhang, X.; Zhang, J.; Liang, S. Nutrient Recovery from Wastewater: From Technology to Economy. *Bioresour. Technol. Rep.* **2020**, *11*, 100425.

(6) Zhang, Y.; Van der Bruggen, B.; Pinoy, L.; Meesschaert, B. Separation of Nutrient Ions and Organic Compounds from Salts in RO Concentrates by Standard and Monovalent Selective Ion-Exchange Membranes Used in Electrodialysis. *J. Membr. Sci.* **2009**, *332*, 104−112.

(7) Borch, T.; Dionysiou, D.; Katz, L.; Xu, P.; Breckenridge, R.; Ellison, K.; Fox, J.; Macknick, J.; Sedlak, D.; Stokes-Draut, J. *National Alliance for Water Innovation (NAWI) Technology Roadmap: Agriculture Sector*; National Renewable Energy Lab. (NREL): Golden, CO (United States), 2021.

(8) Giammar, D.; Jiang, S.; Xu, P.; Breckenridge, R.; Macknick, J.; Rao, N.; Sedlak, D.; Stokes-Draut, J. *National Alliance for Water Innovation (NAWI) Technology Roadmap: Municipal Sector*; National Renewable Energy Lab. (NREL): Golden, CO (United States), 2021.

(9) Grzegorzek, M.; Majewska-Nowak, K.; Ahmed, A. E. Removal of Fluoride from Multicomponent Water Solutions with the Use of Monovalent Selective Ion-Exchange Membranes. *Sci. Total Environ.* **2020**, *722*, 137681.

(10) Kumar, A.; Fukuda, H.; Hatton, T. A.; Lienhard, J. H. Lithium Recovery from Oil and Gas Produced Water: A Need for a Growing Energy Industry. *ACS Energy Lett.* **2019**, *4*, 1471−1474.

(11) Strathmann, H. *Ion-Exchange Membrane Separation Processes*; Elsevier, 2004.

(12) Strathmann, H. Electrodialysis, a Mature Technology with a Multitude of New Applications. *Desalination* **2010**, *264*, 268−288.

(13) Ran, J.; Wu, L.; He, Y.; Yang, Z.; Wang, Y.; Jiang, C.; Ge, L.; Bakangura, E.; Xu, T. Ion Exchange Membranes: New Developments and Applications. *J. Membr. Sci.* **2017**, *522*, 267−291.

(14) Mei, Y.; Tang, C. Y. Recent Developments and Future Perspectives of Reverse Electrodialysis Technology: A Review. *Desalination* **2018**, *425*, 156−174.

(15) Moya, A. A. A Nernst-Planck Analysis on the Contributions of the Ionic Transport in Permeable Ion-Exchange Membranes to the Open Circuit Voltage and the Membrane Resistance in Reverse Electrodialysis Stacks. *Electrochim. Acta* **2017**, *238*, 134−141.

(16) Tedesco, M.; Hamelers, H. V. M.; Biesheuvel, P. M. Nernst-Planck Transport Theory for (Reverse) Electrodialysis: I. Effect of Co-Ion Transport through the Membranes. *J. Membr. Sci.* **2016**, *510*, 370−381.

(17) Yip, N. Y.; Vermaas, D. A.; Nijmeijer, K.; Elimelech, M. Thermodynamic, Energy Efficiency, and Power Density Analysis of Reverse Electrodialysis Power Generation with Natural Salinity Gradients. *Environ. Sci. Technol.* **2014**, *48*, 4925−4936.

(18) Merle, G.; Wessling, M.; Nijmeijer, K. Anion Exchange Membranes for Alkaline Fuel Cells: A Review. *J. Membr. Sci.* **2011**, *377*, 1−35.

(19) Kreuer, K. D. On the Development of Proton Conducting Polymer Membranes for Hydrogen and Methanol Fuel Cells. *J. Membr. Sci.* **2001**, *185*, 29−39.

(20) Luo, T.; Abdu, S.; Wessling, M. Selectivity of Ion Exchange Membranes: A Review. *J. Membr. Sci.* **2018**, *555*, 429−454.

(21) Epsztein, R.; DuChanois, R. M.; Ritt, C. L.; Noy, A.; Elimelech, M. Towards Single-Species Selectivity of Membranes with Sub-nanometre Pores. *Nat. Nanotechnol.* **2020**, *15*, 426−436.

(22) Sujanani, R.; Landsman, M. R.; Jiao, S.; Moon, J. D.; Shell, M. S.; Lawler, D. F.; Katz, L. E.; Freeman, B. D. Designing Solute-Tailored Selectivity in Membranes: Perspectives for Water Reuse and Resource Recovery. *ACS Macro Lett.* **2020**, *9*, 1709−1717.

(23) Tang, C.; Bruening, M. L. Ion Separations with Membranes. *J. Polym. Sci.* **2020**, *58*, 2831−2856.

(24) DuChanois, R. M.; Porter, C. J.; Violet, C.; Verduzco, R.; Elimelech, M. Membrane Materials for Selective Ion Separations at the Water−Energy Nexus. *Adv. Mater.* **2021**, *33*, 2101312.
(25) Bard, A. J.; Faulkner, L. R. *Electrochemical Methods: Fundamentals and Applications*, 2nd ed.; Wiley: New York, 2001.
(26) Baker, R. W. *Membrane Technology and Applications*; John Wiley & Sons, 2012.
(27) Galama, A. H.; Post, J. W.; Cohen Stuart, M. A.; Biesheuvel, P. M. Validity of the Boltzmann Equation to Describe Donnan Equilibrium at the Membrane−Solution Interface. *J. Membr. Sci.* **2013**, *442*, 131−139.
(28) Luo, T.; Roghmans, F.; Wessling, M. Ion Mobility and Partition Determine the Counter-Ion Selectivity of Ion Exchange Membranes. *J. Membr. Sci.* **2020**, *597*, 117645.
(29) Goswami, A.; Acharya, A.; Pandey, A. K. Study of Self-Diffusion of Monovalent and Divalent Cations in Nafion-117 Ion-Exchange Membrane. *J. Phys. Chem. B* **2001**, *105*, 9196−9201.
(30) Geise, G. M.; Hickner, M. A.; Logan, B. E. Ionic Resistance and Permselectivity Tradeoffs in Anion Exchange Membranes. *ACS Appl. Mater. Interfaces* **2013**, *5*, 10294−10301.
(31) Knauth, P.; Pasquini, L.; Narducci, R.; Sgreccia, E.; Becerra-Arciniegas, R.-A.; Di Vona, M. L. Effective Ion Mobility in Anion Exchange Ionomers: Relations with Hydration, Porosity, Tortuosity, and Percolation. *J. Membr. Sci.* **2021**, *617*, 118622.
(32) Shi, S.; Weber, A. Z.; Kusoglu, A. STRUCTURE-TRANSPORT RELATIONSHIP OF PERFLUOROSULFONIC-ACID MEMBRANES IN DIFFERENT CATIONIC FORMS. *Electrochim. Acta* **2016**, *220*, 517−528.
(33) Ueda, T.; Kamo, N.; Ishida, N.; Kobatake, Y. Effective Fixed Charge Density Governing Membrane Phenomena. IV. Further Study of Activity Coefficients and Mobilities of Small Ions in Charged Membranes. *J. Phys. Chem.* **1972**, *76*, 2447−2452.
(34) Hsu, W. Y.; Gierke, T. D. Ion Transport and Clustering in Nafion Perfluorinated Membranes. *J. Membr. Sci.* **1983**, *13*, 307−326.
(35) Zabolotsky, V. I.; Nikonenko, V. V. Effect of Structural Membrane Inhomogeneity on Transport Properties. *J. Membr. Sci.* **1993**, *79*, 181−198.
(36) Schmidt-Rohr, K.; Chen, Q. Parallel Cylindrical Water Nanochannels in Nafion Fuel-Cell Membranes. *Nat. Mater.* **2008**, *7*, 75−83.
(37) Okada, T.; Xie, G.; Gorseth, O.; Kjelstrup, S.; Nakamura, N.; Arimura, T. Ion and Water Transport Characteristics of Nafion Membranes as Electrolytes. *Electrochim. Acta* **1998**, *43*, 3741−3747.
(38) Hongsirikarn, K.; Goodwin, J. G.; Greenway, S.; Creager, S. Effect of Cations (Na+, Ca2+, Fe3+) on the Conductivity of a Nafion Membrane. *J. Power Sources* **2010**, *195*, 7213−7220.
(39) Miyoshi, H. Diffusion Coefficients of Ions through Ion Excange Membrane in Donnan Dialysis Using Ions of Different Valence. *J. Membr. Sci.* **1998**, *141*, 101−110.
(40) Fernandez-Prini, R.; Philipp, M. Tracer Diffusion Coefficients of Counterions in Homo- and Heteroionic Poly(Styrenesulfonate) Resins. *J. Phys. Chem.* **1976**, *80*, 2041−2046.
(41) Zhu, S.; Kingsbury, R. S.; Call, D. F.; Coronell, O. Impact of Solution Composition on the Resistance of Ion Exchange Membranes. *J. Membr. Sci.* **2018**, *554*, 39−47.
(42) Kamcev, J.; Paul, D. R.; Freeman, B. D. Ion Activity Coefficients in Ion Exchange Polymers: Applicability of Manning's Counterion Condensation Theory. *Macromolecules* **2015**, *48*, 8011−8024.
(43) Kamcev, J.; Paul, D. R.; Manning, G. S.; Freeman, B. D. Predicting Salt Permeability Coefficients in Highly Swollen, Highly Charged Ion Exchange Membranes. *ACS Appl. Mater. Interfaces* **2017**, *9*, 4044−4056.
(44) Kamcev, J.; Paul, D. R.; Manning, G. S.; Freeman, B. D. Ion Diffusion Coefficients in Ion Exchange Membranes: Significance of Counterion Condensation. *Macromolecules* **2018**, *51*, 5519−5529.
(45) Tedesco, M.; Hamelers, H. V. M.; Biesheuvel, P. M. Nernst-Planck Transport Theory for (Reverse) Electrodialysis: II. Effect of Water Transport through Ion-Exchange Membranes. *J. Membr. Sci.* **2017**, *531*, 172−182.
(46) Tedesco, M.; Hamelers, H. V. M.; Biesheuvel, P. M. Nernst-Planck Transport Theory for (Reverse) Electrodialysis: III. Optimal Membrane Thickness for Enhanced Process Performance. *J. Membr. Sci.* **2018**, *565*, 480−487.
(47) Biesheuvel, P. M.; Zhang, L.; Gasquet, P.; Blankert, B.; Elimelech, M.; van der Meer, W. G. J. Ion Selectivity in Brackish Water Desalination by Reverse Osmosis: Theory, Measurements, and Implications. *Environ. Sci. Technol. Lett.* **2020**, *7*, 42−47.
(48) Robinson, R. A.; Stokes, R. H. *Electrolyte Solutions*, 2nd ed.; Courier Corporation, 2002.
(49) Mackie, J. S.; Meares, P.; Rideal, E. K. The Diffusion of Electrolytes in a Cation-Exchange Resin Membrane I. Theoretical. *Proc. Roy. Soc. Lond. Math. Phys. Sci.* **1955**, *232*, 498−509.
(50) Mackie, J. S.; Meares, P.; Rideal, E. K. The Diffusion of Electrolytes in a Cation-Exchange Resin Membrane. II. Experimental. *Proc. Roy. Soc. Lond. Math. Phys. Sci.* **1955**, *232*, 510−518.
(51) Amsden, B. Solute Diffusion within Hydrogels. Mechanisms and Models. *Macromolecules* **1998**, *31*, 8382−8395.
(52) Yasuda, H.; Lamaze, C. E.; Ikenberry, L. D. Permeability of Solutes through Hydrated Polymer Membranes. Part I. Diffusion of Sodium Chloride. *Die Makromolekulare Chem.* **1968**, *118*, 19−35.
(53) Debye, P.; HückelDe La Theorie Des Electrolytes, E. I. Abaissement Du Point de Congelation et Phenomenes Associes. *Phys. Z.* **1923**, *24*, 185−206.
(54) Onsager, L. The Motion of Ions: Principles and Concepts. *Science* **1969**, *166*, 1359−1364.
(55) Lifson, S.; Jackson, J. L. On the Self-diffusion of Ions in a Polyelectrolyte Solution. *J. Chem. Phys.* **1962**, *36*, 2410−2414.
(56) Jackson, J. L.; Coriell, S. R. Effective Diffusion Constant in a Polyelectrolyte Solution. *J. Chem. Phys.* **1963**, *38*, 959−968.
(57) Coriell, S. R.; Jackson, J. L. Potential and Effective Diffusion Constant in a Polyelectrolyte Solution. *J. Chem. Phys.* **1963**, *39*, 2418−2422.
(58) Manning, G. S. Nonconvective Ionic Flow in Fixed-Charge Systems. *J. Chem. Phys.* **1967**, *46*, 2324−2333.
(59) Manning, G. S. Limiting Laws and Counterion Condensation in Polyelectrolyte Solutions II. Self-diffusion of the Small Ions. *J. Chem. Phys.* **1969**, *51*, 934−938.
(60) Zwanzig, R. Diffusion in a Rough Potential. *Proc. Natl. Acad. Sci. U.S.A.* **1988**, *85*, 2029−2030.
(61) Berezina, N. P.; Kononenko, N. A.; Dyomina, O. A.; Gnusin, N. P. Characterization of Ion-Exchange Membrane Materials: Properties vs Structure. *Adv. Colloid Interface Sci.* **2008**, *139*, 3−28.
(62) Kamcev, J.; Paul, D. R.; Freeman, D. Effect of Fixed Charge Group Concentration on Equilibrium Ion Sorption in Ion Exchange Membranes. *J. Mater. Chem. A* **2017**, *5*, 4638−4650.
(63) Luo, T.; Zhong, Y.; Xu, D.; Wang, X.; Wessling, M. Combining Manning's Theory and the Ionic Conductivity Experimental Approach to Characterize Selectivity of Cation Exchange Membranes. *J. Membr. Sci.* **2021**, *629*, 119263.
(64) Fan, H.; Yip, N. Y. Elucidating Conductivity-Permselectivity Tradeoffs in Electrodialysis and Reverse Electrodialysis by Structure-Property Analysis of Ion-Exchange Membranes. *J. Membr. Sci.* **2019**, *573*, 668−681.
(65) Suresh, G.; Sodaye, S.; Scindia, Y. M.; Pandey, A. K.; Goswami, A. Study on Physical and Electrostatic Interactions of Counterions in Poly(Perfluorosulfonic) Acid Matrix: Characterization of Diffusion Properties of Membrane Using Radiotracers. *Electrochim. Acta* **2007**, *52*, 5968−5974.
(66) Helfferich, F. G. *Ion Exchange*; Courier Corporation, 1995.
(67) Kingsbury, R. S.; Zhu, S.; Flotron, S.; Coronell, O. Microstructure Determines Water and Salt Permeation in Commercial Ion-Exchange Membranes. *ACS Appl. Mater. Interfaces* **2018**, *10*, 39745−39756.
(68) Tuan, L. X.; Verbanck, M.; Buess-Herman, C.; Hurwitz, H. D. Properties of CMV Cation Exchange Membranes in Sulfuric Acid Media. *J. Membr. Sci.* **2006**, *284*, 67−78.

https://doi.org/10.1021/acsestengg.1c00457
ACS EST Engg. 2022, 2, 1274−1286

(69) High-performance fumasep ion exchange membranes for Electro Membrane Processes. https://www.fumatech.com/NR/rdonlyres/3DF915E1-47B5-4F43-B18A-D23F9CD9FC9D/0/FUMATECH_BWT_GmbHIon_Exchange_Membranes.pdf (accessed Jan 23, 2022).
(70) Hulme, A. M.; Davey, C. J.; Tyrrel, S.; Pidou, M.; McAdam, E. J. Transitioning from Electrodialysis to Reverse Electrodialysis Stack Design for Energy Generation from High Concentration Salinity Gradients. *Energy Convers. Manage.* **2021**, *244*, 114493.
(71) RALEX ion exchange membranes for ED, EDI and E-coating| MEGA. https://www.mega.cz/membranes/(accessed Jan 23, 2022).
(72) Le, X. T.; Bui, T. H.; Viel, P.; Berthelot, T.; Palacin, S. On the Structure−Properties Relationship of the AMV Anion Exchange Membrane. *J. Membr. Sci.* **2009**, *340*, 133−140.
(73) Fan, H.; Huang, Y.; Yip, N. Y. Advancing the Conductivity-Permselectivity Tradeoff of Electrodialysis Ion-Exchange Membranes with Sulfonated CNT Nanocomposites. *J. Membr. Sci.* **2020**, *610*, 118259.
(74) Sata, T. *Ion Exchange Membranes: Preparation, Characterization, Modification and Application*; Royal Society of Chemistry, 2007.
(75) Ji, Y.; Luo, H.; Geise, G. M. Effects of Fixed Charge Group Physicochemistry on Anion Exchange Membrane Permselectivity and Ion Transport. *Phys. Chem. Chem. Phys.* **2020**, *22*, 7283−7293.
(76) Długołęcki, P.; Nymeijer, K.; Metz, S.; Wessling, M. Current Status of Ion Exchange Membranes for Power Generation from Salinity Gradients. *J. Membr. Sci.* **2008**, *319*, 214−222.
(77) Semnani, D. 7—Geometrical Characterization of Electrospun Nanofibers. In *Woodhead Publishing Series in Textiles*; Nanofibers, E., Afshari, M., Eds.; Woodhead Publishing, 2017; pp 151−180.
(78) Długołęcki, P.; Ogonowski, P.; Metz, S. J.; Saakes, M.; Nijmeijer, K.; Wessling, M. On the Resistances of Membrane, Diffusion Boundary Layer and Double Layer in Ion Exchange Membrane Transport. *J. Membr. Sci.* **2010**, *349*, 369−379.
(79) Luo, H.; Chang, K.; Bahati, K.; Geise, G. M. Functional Group Configuration Influences Salt Transport in Desalination Membrane Materials. *J. Membr. Sci.* **2019**, *590*, 117295.
(80) Chang, K.; Luo, H.; Geise, G. M. Water Content, Relative Permittivity, and Ion Sorption Properties of Polymers for Membrane Desalination. *J. Membr. Sci.* **2019**, *574*, 24−32.
(81) Chang, K.; Luo, H.; Bannon, S. M.; Lin, S. Y.; Agata, W.-A. S.; Geise, G. M. Methoxy Groups Increase Water and Decrease Salt Permeability Properties of Sulfonated Polysulfone Desalination Membranes. *J. Membr. Sci.* **2021**, *630*, 119298.
(82) Vanysek, P. Ionic Conductivity and Diffusion at Infinite Dilution. *CRC Handbook of Chemistry and Physics*, 2000; CRC Press, Vol. *83*, pp 76−78.
(83) Logette, S.; Eysseric, C.; Pourcelly, G.; Lindheimer, A.; Gavach, C. Selective Permeability of a Perfluorosulphonic Membrane to Different Valency Cations. Ion-Exchange Isotherms and Kinetic Aspects. *J. Membr. Sci.* **1998**, *144*, 259−274.
(84) Guzmán-Garcia, A. G.; Pintauro, P. N.; Verbrugge, M. W.; Hill, R. F. Development of a Space-Charge Transport Model for Ion-Exchange Membranes. *AIChE J.* **1990**, *36*, 1061−1074.
(85) Nandan, D.; Mohan, H.; Iyer, R. M. Methanol and Water Uptake, Densities, Equivalental Volumes and Thicknesses of Several Uni- and Divalent Ionic Perfluorosulphonate Exchange Membranes (Nafion-117) and Their Methanol-Water Fractionation Behaviour at 298 K. *J. Membr. Sci.* **1992**, *71*, 69−80.
(86) Uematsu, M.; Frank, E. U. Static Dielectric Constant of Water and Steam. *J. Phys. Chem. Ref. Data* **1980**, *9*, 1291−1306.
(87) Chang, K.; Geise, G. M. Dielectric Permittivity Properties of Hydrated Polymers: Measurement and Connection to Ion Transport Properties. *Ind. Eng. Chem. Res.* **2019**, *59*, 5205−5217.
(88) Chang, K.; Luo, H.; Geise, G. M. Influence of Salt Concentration on Hydrated Polymer Relative Permittivity and State of Water Properties. *Macromolecules* **2021**, *54*, 637−646.
(89) Ahmad, Z. Polymer Dielectric Materials. *Dielectric material*; IntechOpen, 2012.
(90) Pintauro, P. N.; Verbrugge, M. W. The Electric-Potential Profile in Ion-Exchange Membrane Pores. *J. Membr. Sci.* **1989**, *44*, 197−212.
(91) Wang, R.; Lin, S. Pore Model for Nanofiltration: History, Theoretical Framework, Key Predictions, Limitations, and Prospects. *J. Membr. Sci.* **2020**, *620*, 118809.
(92) Nightingale, E. R. Phenomenological Theory of Ion Solvation. Effective Radii of Hydrated Ions. *J. Phys. Chem.* **1959**, *63*, 1381−1387.
(93) Díaz, J. C.; Kamcev, J. Ionic Conductivity of Ion-Exchange Membranes: Measurement Techniques and Salt Concentration Dependence. *J. Membr. Sci.* **2021**, *618*, 118718.
(94) Xie, W.; Ju, H.; Geise, G. M.; Freeman, B. D.; Mardel, J. I.; Hill, A. J.; McGrath, J. E. Effect of Free Volume on Water and Salt Transport Properties in Directly Copolymerized Disulfonated Poly(Arylene Ether Sulfone) Random Copolymers. *Macromolecules* **2011**, *44*, 4428−4438.
(95) Galizia, M.; Benedetti, F. M.; Paul, D. R.; Freeman, B. D. Monovalent and Divalent Ion Sorption in a Cation Exchange Membrane Based on Cross-Linked Poly (p-Styrene Sulfonate-Co-Divinylbenzene). *J. Membr. Sci.* **2017**, *535*, 132−142.
(96) Paithankar, D. Y.; Wang, N. H. L. Molecular Simulations of Anion-Exchange Systems: Quaternary Methylammonium Ion Functional Group with Various Anions. *J. Phys. Chem.* **1991**, *95*, 8899−8909.
(97) Clifford, D.; Weber, W. J. The Determinants of Divalent/Monovalent Selectivity in Anion Exchangers. *React. Polym. Ion. Exch. Sorbents* **1983**, *1*, 77−89.
(98) Barron, R. E.; Fritz, J. S. Effect of Functional Group Structure and Exchange Capacity on the Selectivity of Anion Exchangers for Divalent Anions. *J. Chromatogr. A* **1984**, *316*, 201−210.
(99) Tansel, B. Significance of Thermodynamic and Physical Characteristics on Permeation of Ions during Membrane Separation: Hydrated Radius, Hydration Free Energy and Viscous Effects. *Sep. Purif. Technol.* **2012**, *86*, 119−126.
(100) Badessa, T.; Shaposhnik, V. The Electrodialysis of Electrolyte Solutions of Multi-Charged Cations. *J. Membr. Sci.* **2016**, *498*, 86−93.
(101) Boyd, G. E.; Soldano, B. A. Self-Diffusion of Cations in and through Sulfonated Polystyrene Cation-Exchange Polymers1. *J. Am. Chem. Soc.* **1953**, *75*, 6091−6099.
(102) Chaudhury, S.; Agarwal, C.; Pandey, A. K.; Goswami, A. Self-Diffusion of Ions in Nafion-117 Membrane Having Mixed Ionic Composition. *J. Phys. Chem. B* **2012**, *116*, 1605−1611.
(103) Marino, M. G.; Melchior, J. P.; Wohlfarth, A.; Kreuer, K. D. Hydroxide, Halide and Water Transport in a Model Anion Exchange Membrane. *J. Membr. Sci.* **2014**, *464*, 61−71.
(104) Epsztein, R.; Shaulsky, E.; Qin, M.; Elimelech, M. Activation Behavior for Ion Permeation in Ion-Exchange Membranes: Role of Ion Dehydration in Selective Transport. *J. Membr. Sci.* **2019**, *580*, 316−326.
(105) Zhou, X.; Wang, Z.; Epsztein, R.; Zhan, C.; Li, W.; Fortner, J. D.; Pham, T. A.; Kim, J. H.; Elimelech, M. Intrapore Energy Barriers Govern Ion Transport and Selectivity of Desalination Membranes. *Sci. Adv.* **2020**, *6*, No. eabd9045.
(106) Lu, C.; Hu, C.; Ritt, C. L.; Hua, X.; Sun, J.; Xia, H.; Liu, Y.; Li, D.-W.; Ma, B.; Elimelech, M.; Qu, J. In Situ Characterization of Dehydration during Ion Transport in Polymeric Nanochannels. *J. Am. Chem. Soc.* **2021**, *143*, 14242−14252.
(107) Kamcev, J.; Galizia, M.; Benedetti, F. M.; Jang, E.-S.; Paul, D. R.; Freeman, B. D.; Manning, G. S. Partitioning of Mobile Ions between Ion Exchange Polymers and Aqueous Salt Solutions: Importance of Counter-Ion Condensation. *Phys. Chem. Chem. Phys.* **2016**, *18*, 6021−6031.
(108) Münchinger, A.; Kreuer, K.-D. Selective Ion Transport through Hydrated Cation and Anion Exchange Membranes I. The Effect of Specific Interactions. *J. Membr. Sci.* **2019**, *592*, 117372.
(109) Cassady, H. J.; Cimino, E. C.; Kumar, M.; Hickner, M. A. Specific Ion Effects on the Permselectivity of Sulfonated Poly(Ether Sulfone) Cation Exchange Membranes. *J. Membr. Sci.* **2016**, *508*, 146−152.

https://doi.org/10.1021/acsestengg.1c00457
ACS EST Engg. 2022, 2, 1274−1286

(110) White, N.; Misovich, M.; Yaroshchuk, A.; Bruening, M. L. Coating of Nafion Membranes with Polyelectrolyte Multilayers to Achieve High Monovalent/Divalent Cation Electrodialysis Selectivities. *ACS Appl. Mater. Interfaces* **2015**, *7*, 6620−6628.
(111) Le, X. T.; Viel, P.; Jégou, P.; Garcia, A.; Berthelot, T.; Bui, T. H.; Palacin, S. Diazonium -Induced Anchoring Process: An Application to Improve the Monovalent Selectivity of Cation Exchange Membranes. *J. Mater. Chem.* **2010**, *20*, 3750−3757.

https://doi.org/10.1021/acsestengg.1c00457
ACS EST Engg. 2022, 2, 1274−1286